BGSG

Volume 55

Research Paper

Correspondence to:
Panayota Makri
pmakri@geol.uoa.gr

DOI number:
http://dx.doi.org/10.12681/bgsg.20938

Keywords:
coastal aquifer, hydrochemistry, seawater intrusion, Thriassion Plain

Citation:
Panayota Makri, Dimitrios Hermides, Maria Psychogiou, Aikaterini Ermidou (2019), The use of geochemical ratios in groundwater quality assessment: the case of the Thriassion Plain, Attica, Greece. Bulletin Geological Society of Greece, 55, 223-240.

Publication History:
Received: 29/07/2019
Accepted: 11/11/2019
Accepted article online: 06/12/2019

The Editor wishes to thank two anonymous reviewers for their work with the scientific reviewing of the manuscript and Ms Erietta Vlachou for editorial assistance

©2019. The Authors
This is an open access article under the terms of the Creative Commons Attribution License, which permits use, distribution and reproduction in any medium, provided the original work is properly cited

THE USE OF GEOCHEMICAL RATIOS IN GROUNDWATER QUALITY ASSESSMENT: THE CASE OF THE THRIASSION PLAIN, ATTICA, GREECE

Panayota Makri[1*], Dimitrios Hermides[2], Maria Psychogiou[2], Aikaterini Ermidou[2]

[1] Department of Geology and Geoenvironment, National and Kapodistrian University of Athens. E-mail: *pmakri@geol.uoa.gr* ,
[2] Department of Natural Resources Management and Agricultural Engineering, Agricultural University of Athens.
E-mail: *dermides@aua.gr* *lhyd4psm@aua.gr* *katermidou@gmail.com*

Abstract

This paper is an effort to assess the groundwater quality and the geochemical processes mainly using the Chadha's diagram which classifies natural waters and documents the Piper and extended Durov diagrams. Chadha's diagram is a useful tool to interpret groundwater geochemical processes because it is produced by simple spreadsheets excel files. The example of hydrochemical analyses were given from groundwater samples of the Thriassion Plain. To attend our objective, 38 groundwater samples were collected. Hydrochemical sections, XY diagrams, distribution maps of ionic ratios as well as the Gibbs diagrams were used to identify origin of salinity and the hydrogeochemical processes that have taken place. The Gibbs diagrams have shown that evapotranspiration (ET) and rock-water interaction play an important role to the increase of groundwater salinity. The interpretation of Chadha diagram highlights that the stratigraphic factors and especially the clay strata occurrence have isolated fresh groundwater from seawater. The abundant occurrence of clay deposits to the depth of the plain work as barriers to direct seawater intrusion. Good quality groundwater identified confirms the important role of clay strata. Reverse cation exchange, is the predominant geochemical process in the Thriassion Plain aquifers, whereas evapotranspiration (ET) and

rock-water interaction play an important role to the increase of groundwater salinity.

Keywords: *coastal aquifer, hydrochemistry, seawater intrusion, Thriassion Plain*

Περίληψη

Στο άρθρο αυτό γίνεται αρχικά μία εκτίμηση της ποιότητας του υπόγειου νερού, με ταυτόχρονη ταξινόμησή του καθώς και μία μελέτη των γεωχημικών διεργασιών που λαμβάνουν χώρα εντός του υδροφόρου ορίζοντα με τη χρήση του διαγράμματος Chadha, το οποίο βασίζεται αλλά και συμπληρώνει τα διαγράμματα Piper και expanded Durov. Το διάγραμμα του Chadha είναι ένα πολύ χρήσιμο εργαλείο στην ερμηνεία των υδρογεωχημικών διεργασιών στον υπόγειο υδροφορέα καθώς εξάγεται από ένα απλό υπολογιστικό φύλλο αποφεύγοντας τα πολύπλοκα λογισμικά. Τα δεδομένα της εργασίας αυτής προήλθαν από 38 δείγματα υπόγειου νερού στο Θριάσιο Πεδίο. Για να μελετηθεί διεξοδικά η προέλευση της αλατότητας που προσδιορίστηκε στα δείγματα αυτά, και ταυτόχρονα οι υδρογεωχημικές διεργασίες που επιτελούνται, αρχικά χρησιμοποιήθηκαν χάρτες κατανομής των λόγων των ανιόντων και των κατιόντων και διαγράμματα του Gibbs. Από αυτά προέκυψε ότι η εξατμισοδιαπνοή και η αλληλεπίδραση του νερού με τα περιβάλλοντα πετρώματα παίζουν βασικό ρόλο στην αύξηση της αλατότητας. Κατόπιν, από τα παραγόμενα διαγράμματα του Chadha συμπεραίνεται ότι οι σχηματισμοί και ειδικά τα αργιλικά πετρώματα είναι υπεύθυνα για τη δημιουργία ενός φυσικού εμποδίου στην άμεση διείσδυση του θαλάσσιου νερού, συμπέρασμα που επιβεβαιώνει η ύπαρξη νερού χαμηλής αλατότητας στο κεντρικό τμήμα του πεδίου.. Συμπερασματικά, η κύρια γεωχημική διαδικασία που παρατηρείται με τη μελέτη του διαγράμματος Chadha είναι η αντίστροφη κατιοντοανταλλαγή η οποία συνεργεί μαζί με την εξατμισοδιαπνοή και με το είδος των σχηματισμών στην αυξημένη αλατότητα των υπόγειων νερών της περιοχής.

Λέξεις κλειδιά: *παράκτιος υδροφορέας, υδροχημεία, διείσδυση θαλάσσιου νερού, Θριάσιο Πεδίο*

1. Introduction

Hydrochemistry in coastal aquifers is very often influenced by seawater. Natural and anthropogenic factors are the cause of that phenomenon. However, Thriassion Plain seems to retain its good quality groundwater in the central part of the basin due to the occurrence of thick clay strata that prevent seawater intrude inland. The agricultural and industrial water needs in the region are covered by more than 5.000 wells tapping the Plio-Pleistocene sediments and the Mesozoic carbonate. Numerous groundwater studies since 1945 have been accomplished. During the last five decades, the uncontrolled industrial development has resulted to environmental degradation onto the soil, seawater and groundwater (Kaminari, 1994; Kounis and Siemos, 1990; Dounas and Panagiotides, 1964; Dimitriou et al. 2011, Iliopoulos et al. 2010; Christides et al. 2011; Lioni et al. 2008; Makri, 2008; Mimides, 2002). Seawater intrusion has also been studied; high levels of salinity in locations far from the shoreline was better documented by Hermides and Stamatis (2017), who demonstrated that the origin of brackish groundwater is potentially attributed to rock dissolution or anthropogenic factors, studying the halogens ratios and not only the individual concentrations. The target of this work is to further explain the hydro-geochemical processes occurring within the aquifer of Thriassion Plain, which, in turn, may provide useful data about the quality of the groundwater.

2. Study area

Thriassion Plain is a coastal area located 25 km west of Athens. It covers a surface of 100 km^2 which is part of three hydrological basins with total extent of 480 km^2 (Fig. 1). Semi –arid conditions prevail in the area: the mean annual precipitation is 380 mm while evapotranspiration is 68% of the precipitation (Paraschoudes, 2002). In the 2000's, agricultural lands had an extent of about 70 km^2. Half of this surface was irrigated and mainly covered the central part of the study area, whereas, the rest was occupied by urban and industrial activities.

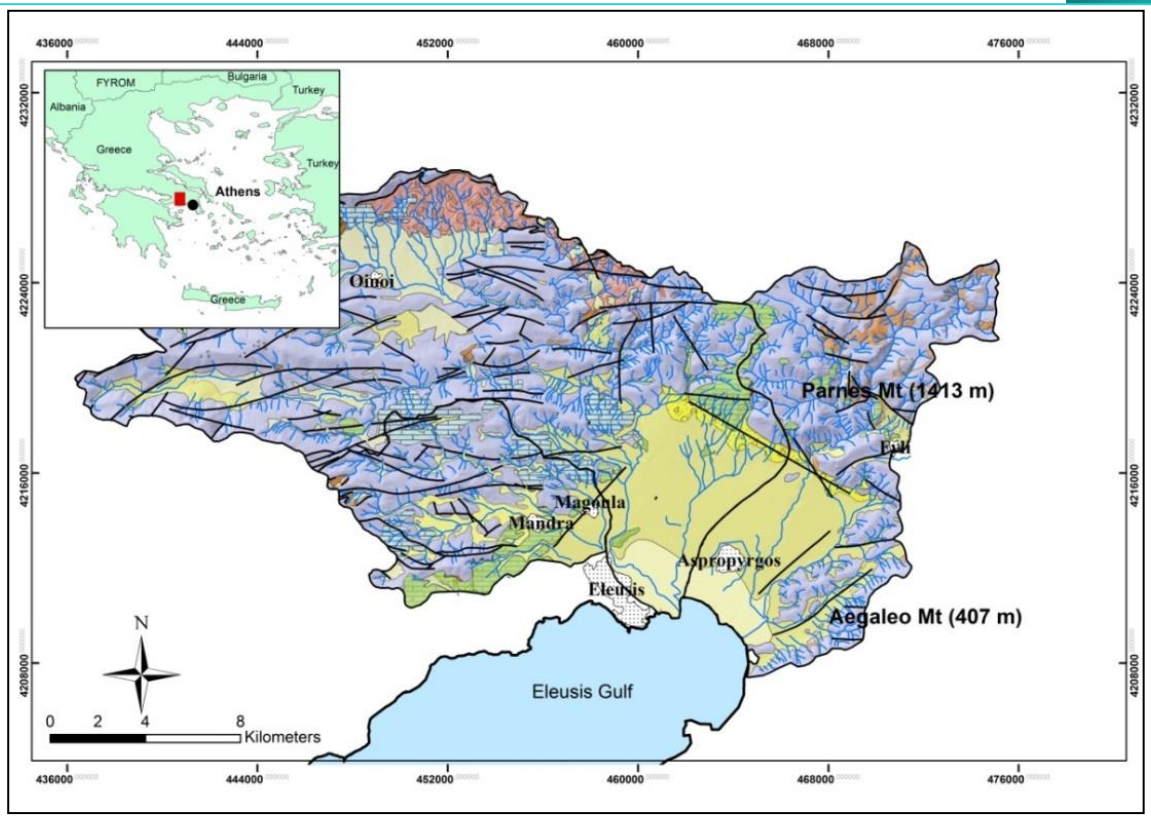

Fig. 1: The broader study area and its hydrological basins

3. Geological setting

The geological background of Thriassion Plain is dominated by sediments and volcanic rocks of Palaeozoic to Caenozoic age (Katsikatsos et al., 1986; Dounas, 1971) (Fig. 2). The Palaeozoic basement is represented by a volcano-sedimentary complex consisted of (a) clastic materials, shales and sandstones; (b) basic igneous volcanic rocks; and (c) lenticular intercalations of thin-bedded carbonate units. These rocks are overlain by Mesozoic sediments comprising of: (a) phyllites and sandstone which mainly consist of: slightly metamorphic schists and sandstone with intercalations of red thin-bedded limestone–dolomites (Phase Hallstatt); (b) metapyroclastic and metavolcanic rocks hornstones and tuffs; (c) Triassic limestones, dolomitic limestones and dolomites; and (d) Cretaceous limestones. Cenozoic sediments in the area consist of: (a) Paleocene flysch; (b) Neogene deposits of Pliocene (marls with lignite intercalations in places, sandstone, marly limestone); and (c) Quaternary deposits of Pleistocene (clay, sands, gravels, torrential fans of loosely and cohesive conglomerates) and alluvial deposits (clays, loams, sands and gravels)

at the top. The geological structure of the narrow area of Thriassion Plain is very complex, due to different sedimentary environments and facies alternations of torrential, lacustrine and lagoon sediments deposited during Neogene–Quaternary period as well as the effects of tectonic and neotectonic deformation (Mariolakos et al., 2001; Ganas et al, 2004; Foumelis, 2019). This structure has influenced the geomorphological, hydrological and hydrogeological characteristics of the above-mentioned area. Clay, marls, consolidated conglomerates, thick-bedded massive limestone, dolomites and shales control the groundwater flow.

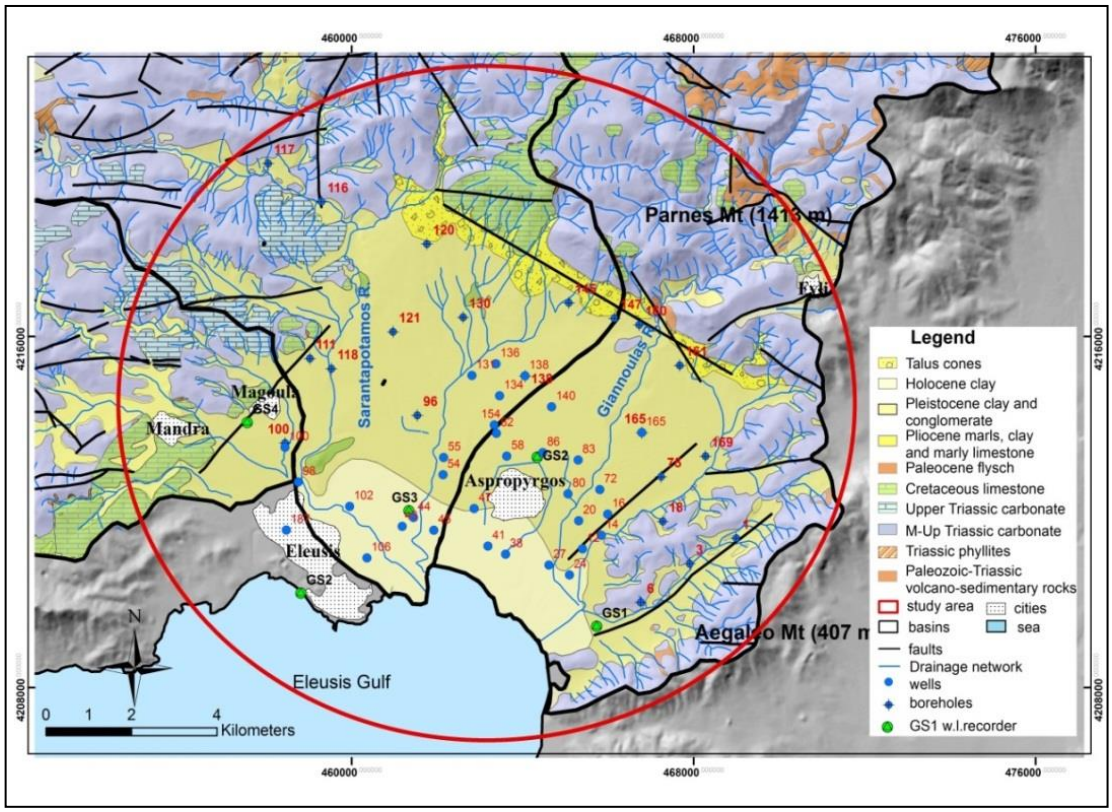

Fig. 2: Geological map of the study area and sampling points

4. Hydrogeological setting

Hydrogeology has been influenced significantly by stratigraphic and tectonic factors (Goumas, 2006; Zacharias et al., 2003; Mariolakos and Theocharis, 2001; Katsikatsos et al., 1986; Dounas, 1971) and by sea level changes (Lambeck, 1996; Kambouroglou, 1989; Kraft et al., 1980). The main aquifers in Thriassion Plain are the Plio–Pleistocene sediments as well as the Triassic

limestone/dolomite and the Cretaceous limestone. Plio– Pleistocene sediments form a multi-layered confined system (Hermides, 2018). This system has clay or marls as a local basement. The geometry of the deposits cannot be described in details, or their total depth, which is likely to be about 300 m (Skianis and Noutsis, 2008). Conversely, carbonates have Palaeozoic sediments as a basement. Potentiometric surface and water table generally fluctuate between the highest level in April– May and the lowest in October. Seasonal water level fluctuations in the unconfined aquifer are about 0.4–0.5 m and about 1.2–1.5 m in the confined aquifers. The upper aquifer is comprised of sediments of Upper Pleistocene to Holocene age that include clays, sands, gravels and pebbles, often forming breccia–conglomerate banks with low groundwater yields. The upper aquifer is generally unconfined and locally confined (Hermides et al., 2016). Holocene clays occur in the coastal area and provide confined conditions. The aquifer has thickness 2–10 m which thickens up to 20–30 m at higher elevation. The hydraulic conductivity ranges between 0.4 and 4 m/d and the pumping rate ranges between 5 and 20 m^3 /h. Groundwater generally flows southwards with a hydraulic gradient of 1 to 3%. Holocene clays locally form barriers to groundwater flow causing an upward leakage. The second aquifer is made up of Lower Pleistocene sediments comprised of clays, sands, gravels and conglomerates. It is confined and forms a multi-layered confined system. Three to five or six aquifers exist in these sediments (Hermides, 2018). The thickness of the aquifers is typically 1–3 m and may be up to 12–15 m in thickness. The third aquifer is made up of Plio–Pleistocene sediments comprised of marls with lignite layers in places, sands and marly limestones. Recharge is achieved from Pleistocene sediments leakage and lateral flow from carbonate. The hydraulic conductivity of this aquifer ranges from 2 to 25 m/d and hydraulic head is up to 13 m amsl. Groundwater in this aquifer flows towards the coast with a hydraulic gradient of 1–5%. The Cretaceous limestone is fractured and forms an unconfined aquifer of high productivity. The quality of water in this aquifer is degraded because of sea water intrusion. The aquifer has a transmissivity of up to 5000 m^2 /d (Kounis and Siemos, 1990) and the pumping rate from individual wells is over 90–100 m^3 /h. The hydraulic gradient in the aquifer is about 0.5–0.6% and the head is up to 7–8 m amsl. The Triassic aquifer is either confined or unconfined depending on its location and tectonism and karstification. A conceptual model of the formations, along with the boreholes and the sampling

wells are depicted in Figure 3, where the dashed line is a very general illustration of the aquifer and the black arrows is the overall groundwater flow.

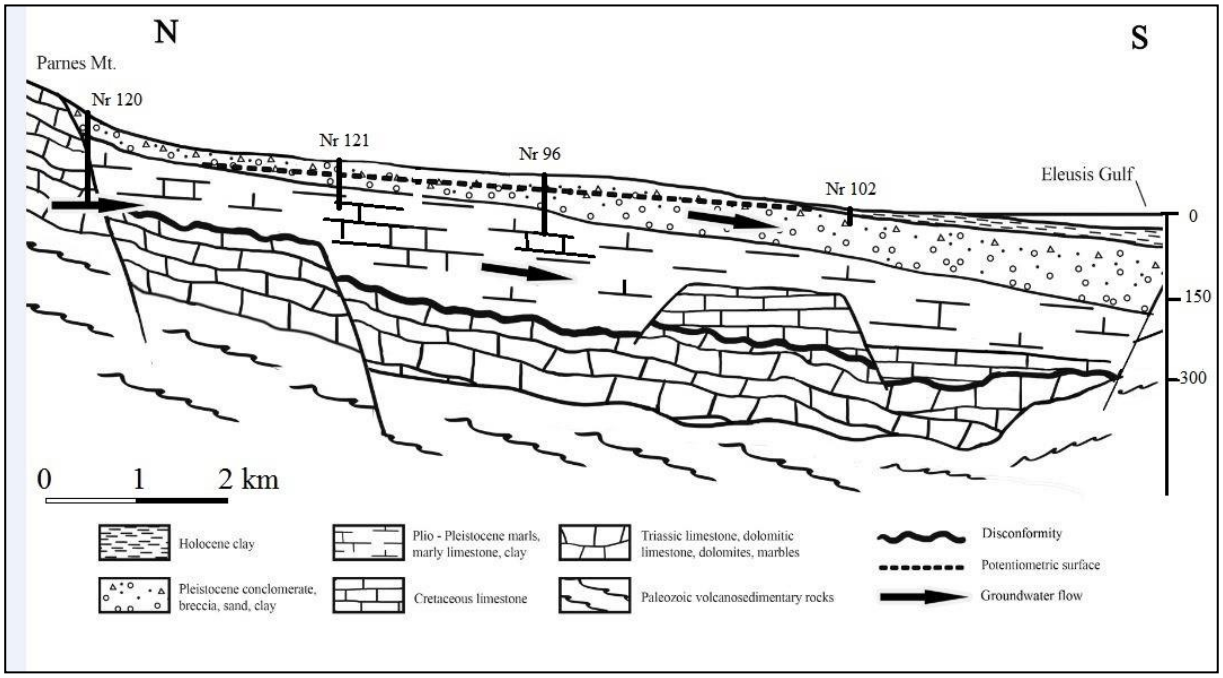

Fig. 3: Conceptual model of the geological strata of the study area in combination with the general groundwater flow.

5. Materials and methods

Water sampling from 38 wells and boreholes along with measurement of basic physico-chemical parameters took place in April/May and in October 2012. Sampling and storage followed the Technical Regulations of International Standards. All sample bottles were cleaned with nitric acid prior to sample collection. Water samples were collected in a 1-l plastic bottle which was rinsed three times prior to sample collection. The average analytical precision was better than 5%. The target anions Cl^-, SO_4^{2-} and cations Ca^{2+}, Mg^{2+}, Na^+, K^+, were determined with Ion Chromatography, while the method of titration was used for HCO_3^- determination. The results were illustrated on the Chadha diagram (Chadha, 1999), XY diagrams, and distribution maps of ionic ratios as well as Gibbs diagrams (Gibbs, 1971). Chadha diagram uses simple spreadsheets excel files for identifying geochemical processes that could take place in groundwater.

Table 1: Physico-chemical parameters of groundwater samples.

A/A	well Nr	Cl^-	NO_3^-	SO_4^{2-}	HCO_3^-	Na^+	K^+	Ca^{2+}	Mg^{2+}	pH	Redox	E.C.	T °C	% balance
1	14A	1740	245	314	296	702	1.0	336	145	7.09	132	5250	21.2	4.4
2	16	280	102	54	300	150	3.7	111	54	7.55	198	1430	20.8	2.9
3	18A	1450	28	151	445	709	16.0	137	105	7.23	91	3980	20.5	3
4	20	773	136	218	331	313	9.6	198	132	7.58	90	2920	21.7	0.6
5	24	1338	68	225	488	798	29.1	189	118	6.95	122	4380	22.7	3
6	27	1134	82	209	404	611	13.0	178	82	7.3	144	3620	21.5	2.1
7	41'	437	182	189	680	429	9.4	182	69	7.59	128	2450	21.5	4.1
8	43'	1252	49	156	285	658	28.0	102	84	7.62	121	3810	22.8	3.2
9	44	484	26	88	357	322	20.7	80	54	8.04	119	1849	22.5	1.3
10	45	2547	152	391	360	1400	40.2	247	178	7.46	131	7660	22.5	0.2
11	47	2920	275	255	253	806	47.4	548	354	7.42	148	8090	21.1	2.3
12	54	328	180	124	433	345	15.6	78	50	7.52	130	1883	20.4	3.2
13	55	103	188	76	374	103	8.2	109	56	7.46	111	1131	20.6	3.4
14	62	227	334	46	231	42	4.5	147	84	7.55	119	1435	20.5	1.9
15	72	291	170	54	296	93	6.3	135	82	7.47	131	1578	21.4	1.7
16	75	159	320	86	314	48	8.5	174	82	7.3	97	1501	21.5	3.1
17	83	366	89	63	237	213	6.8	97	45	7.54	135	1538	21.5	2.2
18	86	304	281	60	261	58	4.6	179	88	7.51	196	1667	20.8	0.4
19	96	461	94	64	709	174	4.0	155	156	7.11	28	2270	21.2	1
20	98	357	42	84	487	188	13.8	159	63	7.25	119	1812	20.3	2.8
21	100	189	173	42	415	66	3.0	191	61	7.4	125	1411	21	4.7
22	102	927	180	156	517	588	14.3	173	116	6.93	136	3630	20.2	3.8
23	106	1639	122	294	444	857	30.3	247	131	7.19	126	5010	21.1	0.7
24	111	658	87	86	318	249	11.3	200	61	7.33	39	2320	20.1	1.9
25	116	300	45	62	360	157	9.2	135	41	7.69	122	1378	21.1	1.8
26	118	1520	28	164	294	728	21.9	166	99	7.47	56	4500	18.3	3.2
27	121	46	60	11	293	28	3.7	61	41	7.92	63	595	18.6	2.6
28	130	489	175	121	226	235	8.2	158	55	7.64	78	2086	17.5	0.3
29	131	193	359	63	292	49	12.5	158	91	7.44	106	1481	20	0.5
30	134	110	377	73	275	50	2.2	150	88	7.47	97	1388	19.5	1.7
31	136	348	157	41	239	82	3.3	153	89	7.55	92	1586	20	3.5
32	138	245	74	11	274	44	2.0	130	53	7.83	44	1104	19.3	5.0
33	140	77	165	54	183	27	4.6	91	45	7.95	95	810	20	2.2
34	147	586	13	79	306	317	12.2	77	56	7.68	-23	2115	18.1	2.1
35	154	117	465	63	270	46	2.5	156	85	7.48	115	1438	20.3	0.6
36	162	40	103	20	232	26	2.3	73	32	8.01	195	570	20	2
37	169	439	35	60	575	291	12.3	178	12	7.28	7	2270	20.2	1.8
38	187	440	44	72	301	233	13.9	97	54	7.31	158	1762	20.3	0.3
	min	40	13	11	183	26	1.0	61	12	6.93	-23	570	17.5	
	max	2920	465	391	709	1400	47.4	548	354	8.04	198	8090	22.8	
	stdev	688	113	90	122	320	10.8	84	57	0.26	48	1760		

Eight (8) fields are presented on a Cartesian system of axes which forms a rectangular. Concentration meq/l % of (Ca^{2+} +Mg^{2+})- (Na^{+} +K^{+}) and HCO_3^-- (Cl^- +SO_4^{2-}) are displayed onto X and Y axes respectively. Fresh waters are projected in the field 5 and reverse cation exchange is dominating in the field 6, whereas seawater influence is depicted in the field 7. Base cation exchange is depicted in the field 8. Fields 1-4 are depicted on the main axes of the Cartesian system.

6. Results and discussion

All data of Table 1 were illustrated on a Chadha diagram (Fig. 4) to interpret groundwater geochemical processes that take place in the Thriassion Plain groundwaters. Mix of fresh water with seawater occurs along the dashed line, while refreshing is depicted with the arrow 1 (samples 41, 44, and 54). These wells are located in the coastal zone and are considered to have been influenced by seawater.

Due to the increased rainfall during 2011-2012 (Hermides, 2018) water has been freshened and base cation-exchange has started. Mix of fresh water with aged water and possible seawater influence may indicate the projection of samples 12, 14A, 20, 38, 47, 80, 130 (arrow 2). These wells tap the aquifer in the Pleistocene sediments and are fed from the rain while some of them have been abandoned and are not in use. Well 130 taps the aquifer in the Cretaceous limestone and it seems to be influenced by seawater. In all previous samples reverse cation exchange takes place. The arrow 3 indicates that wells which are close to the dashed line have been influenced by modern seawater. In the wells 62, 80, 100, 128, 131, 136 and 140 reverse cation exchange takes place (arrow 4). Some of them alternate their position between fields 5 and 6 according to dry or wet season. This means that when fresh water inserts the aquifer from the rain during the wet period, they are projected in field 5 and they return into field 6 during dry period. It may also indicate that the groundwater is related to reverse cation-exchange of old water which exists in the aquifer.

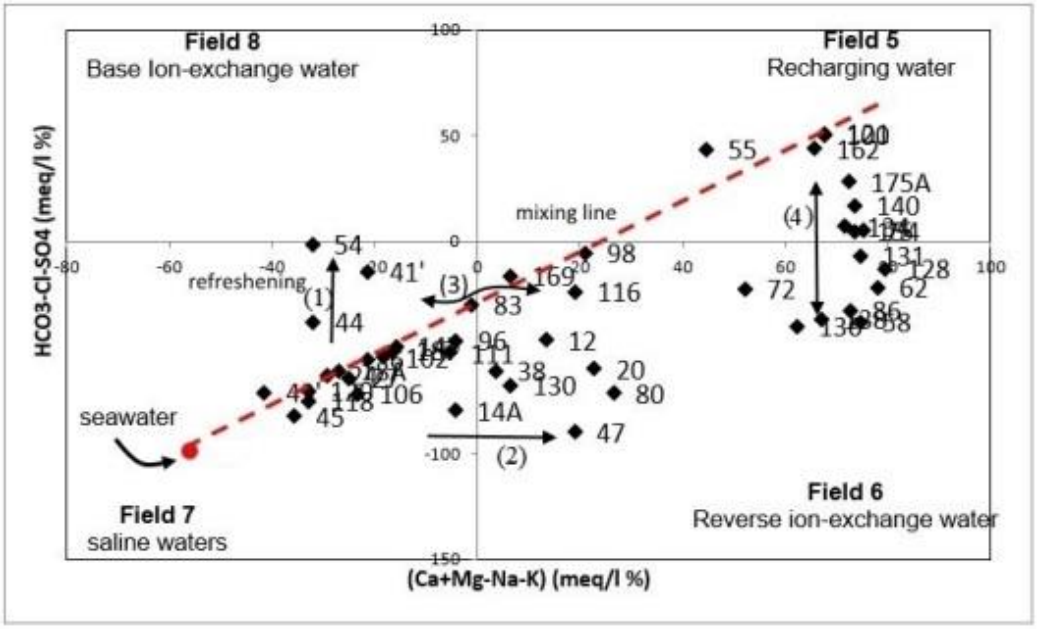

Fig. 4: Chadha diagram based on meq/l% concentrations of major constituents. In the field 5 recharging waters are depicted and in the field 6 reverse-cation exchange takes place. Field 7 represents waters that have been influenced by seawater. The dashed line represents mixing of seawater with fresh water. The numbered lines represent grouping as follows: 1 refreshening; 2 and 4 reverse cation exchange; 3 carbonate waters; those samples that lie on the dashed line are influenced by modern seawater and those samples that are around the dashed line represent old seawater.

The interpretation of the produced diagram highlights the stratigraphic factors and especially the clay strata occurrence that have isolated fresh groundwater from seawater. The abundant occurrence of clay deposits to the depth of the plain work as barriers to sea intrusion. Good quality groundwater identified in the wells close to arrow 4 confirms the role of clay strata. This means that the distinguished two groups of the samples the first near the arrow 4 and the second near the arrow 2 are separated from one another by clay strata. However, in sites, seawater intrudes inland through limestone and buried valleys or where coarse material prevails in the deposits (Paraschoudes, 2002; Kounis and Siemos, 1990). To identify the origin of salinity and other geochemical processes based on the relationship between TDS (meq/l) and $Na^+/(Na^+ + Ca^{2+})$, $Cl^-/(Cl^- + HCO_3^-)$ meq/l ratios, Gibbs diagrams (Fig. 5) have shown that evapotranspiration (ET) and rock-water interaction play an important role to the increase of groundwater

salinity which is in accordance with the Cl^-/Br^- mass ratio reported by Hermides and Stamatis (2017) who have shown that the repeated irrigation water results in increased salinity content of the return water to the aquifers. In Figure 6, XY diagrams show that cation exchange processes are in progress in the Thriassion aquifers. Calcium and magnesium are in excess of bicarbonate sulphates. This means that even more cations have been produced and the reason is not the bicarbonate salts and gypsum/anhydrite dissolution but reverse cation exchange of Na for Ca. This is confirmed in Figure 6b which shows the negative correlation between calcium and magnesium against sodium.

Moreover, high correlation between the sulphates and sodium (Fig. 7) may indicate dissolution of evaporites relics although the latter ones have not been recognized in the study area. Maps distribution of the $(Ca^{2+}+Mg^{2+})/(HCO_3^- +SO_4^{2-})$, $(Ca^{2+}+Mg^{2+})/Na^+$ and Na^+/Cl^- ratios in meq (Fig. 8a, b, c) clearly show the spatial distribution of reverse cation exchange processes, the good water distribution in the central part of the plain and the refreshening processes respectively. Moreover, high correlation between the sulphates and sodium may indicate dissolution of evaporites relics although the latter ones have not been recognized in the study area.

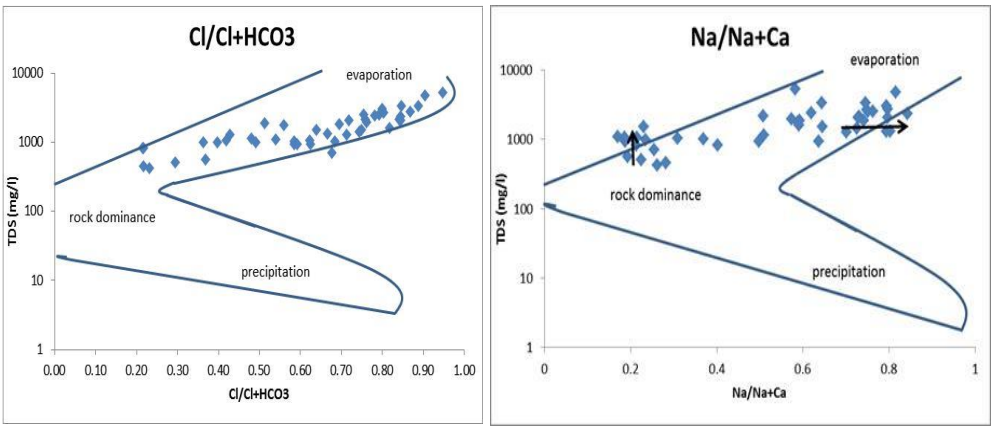

a **b**

Fig. 5: (a, b) Gibbs diagrams showing rock-water interaction and evapotranspiration processes. The arrows show evolutionary paths of groundwater.

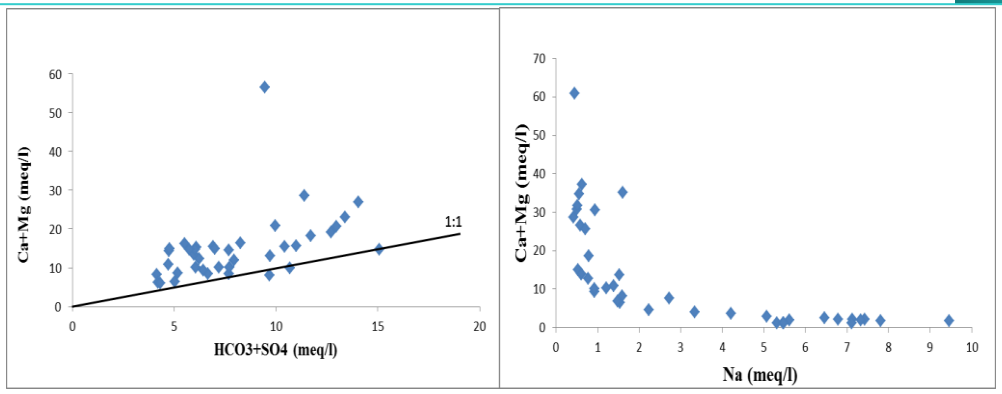

a **b**

Fig. 6: XY diagrams showing cation exchange in progress; a) most of Ca^{2+}nd Mg^{2+} are depicted over the 1:1 line which means that those elements are in excess of bicarbonate and sulphates and b) negative correlation is between concentration of Ca^{2+}+ $Mg^{2+}$and Na^{+} which means that cation exchange processes take place.

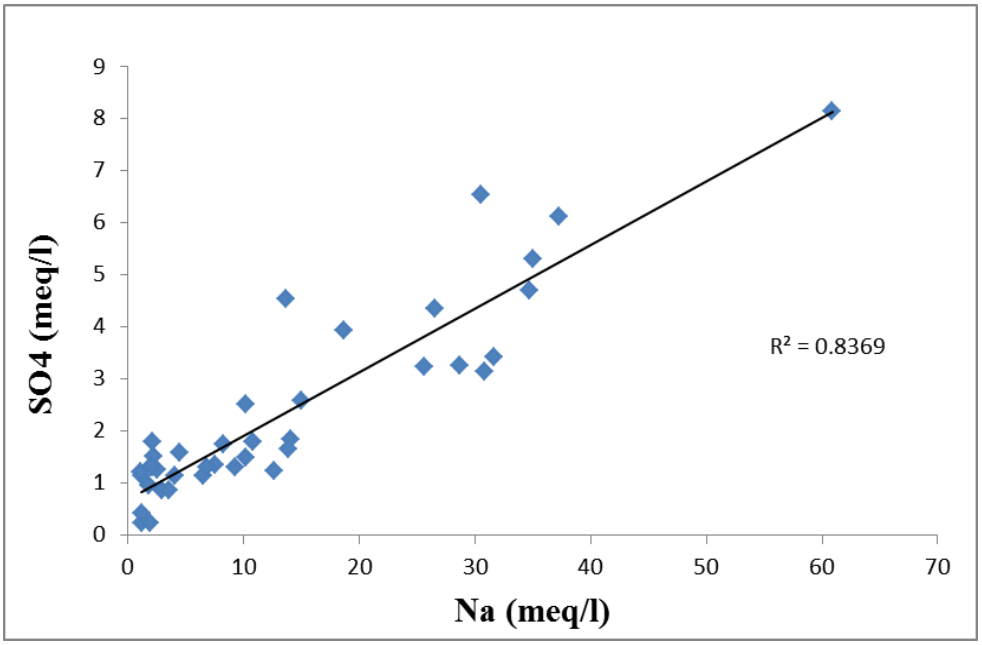

Fig. 7: Diagram showing high positive correlation between sulphates and sodium indicates relics of evaporates.

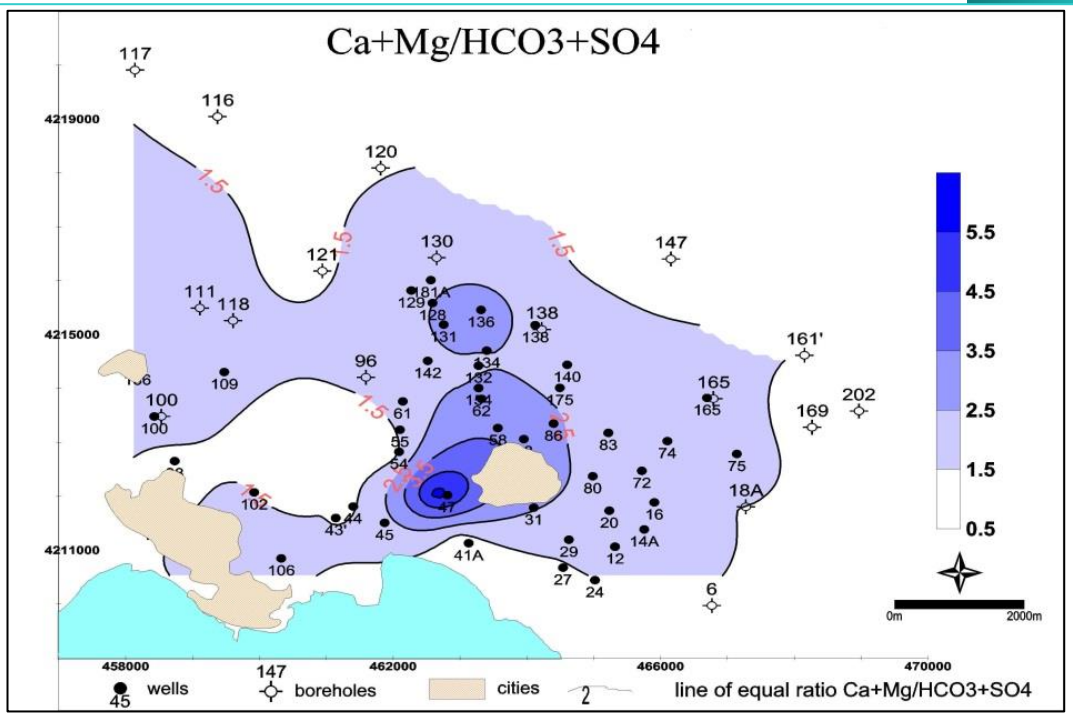
Ca+Mg/HCO3+SO4
4219000
4215000
4211000
458000
462000
466000
470000
5.5
4.5
3.5
2.5
1.5
0.5
0m
2000m
wells
boreholes
cities
line of equal ratio Ca+Mg/HCO3+SO4

8a

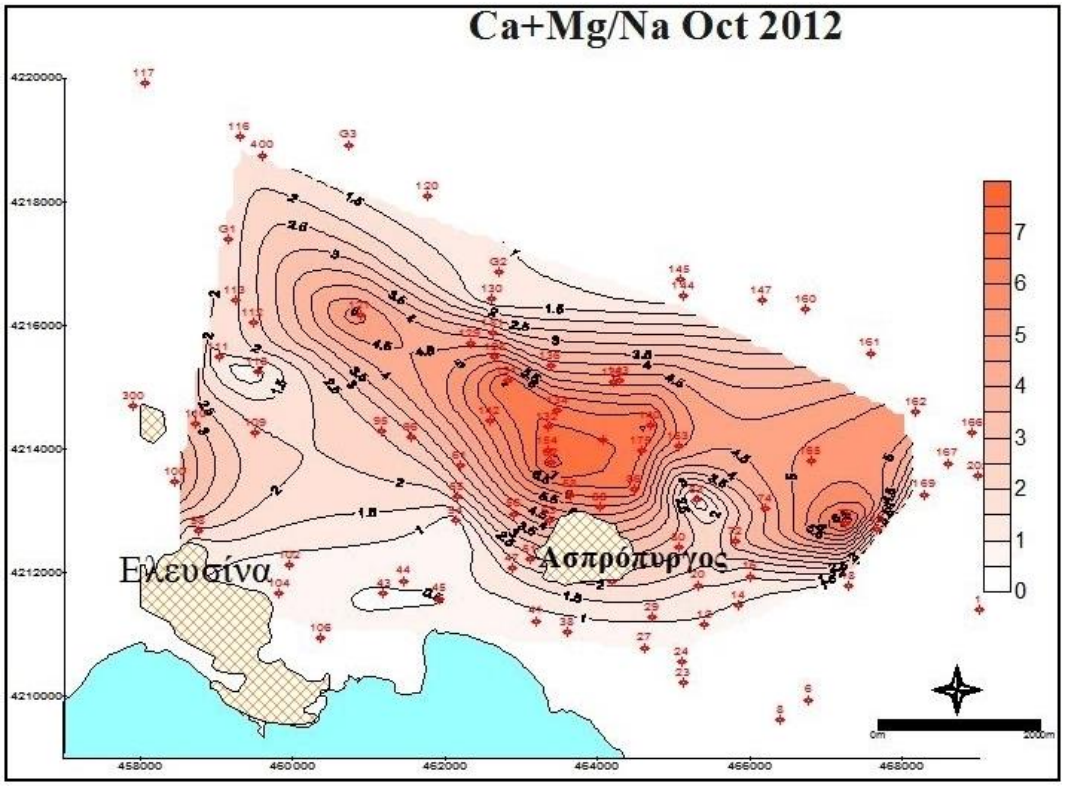
Ca+Mg/Na Oct 2012
4220000
4218000
4216000
4214000
4212000
4210000
458000
460000
462000
464000
466000
468000
Ελευσίνα
Ασπρόπυργος
7
6
5
4
3
2
1
0

8b

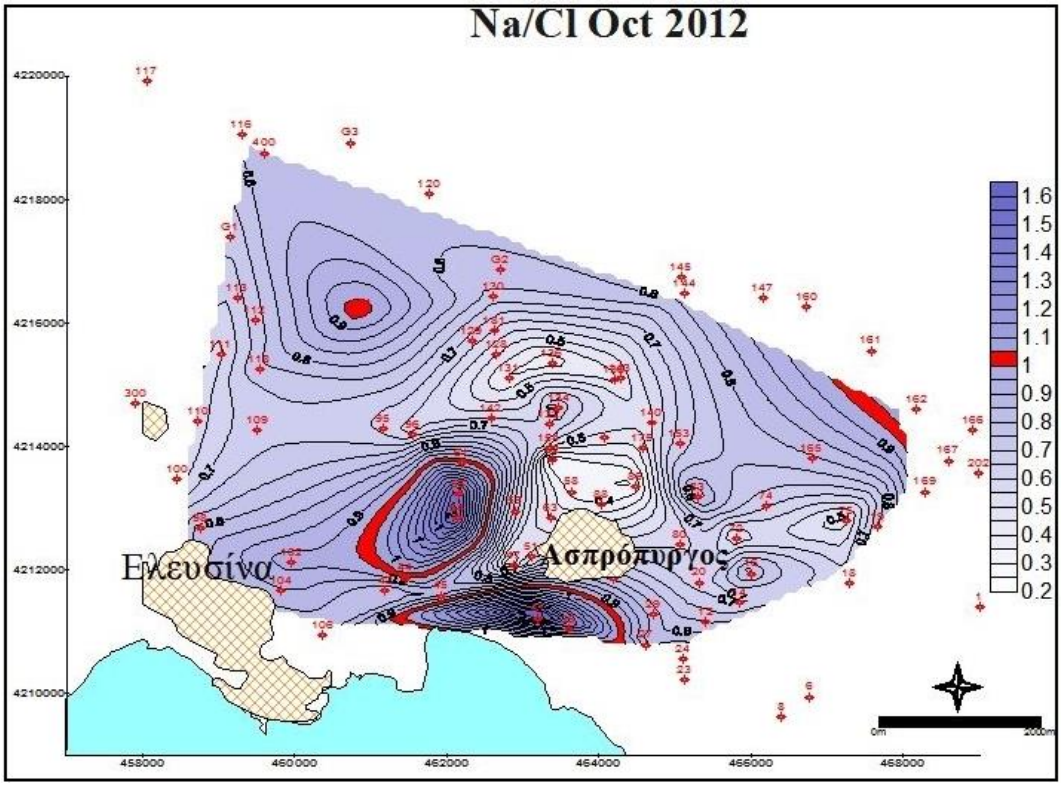

8c

Fig. 8: Distribution maps of a) $Ca^{2+}+Mg^{2+}/HCO_3+SO_4^{2-}$; b) $Ca^{+2}+Mg^{2+}/Na^{+}$; and c) Na^{+}/Cl^{-} ratios in meq. The Na^{+}/Cl^{-} ratio in coastal area far exceeds 1, indicating refreshening processes.

7. Conclusions

This article is an effort to understand the hydrogeochemical processes that take place in the Thriassion Plain aquifers of Western Attica, based on the Chadha diagram. The Chadha diagram resulted in the following thoughts: Mix of fresh water with aged water and possible seawater influence occurs in the Pleistocene aquifer. Reverse cation exchange of Na^{+} for Ca^{2+} is the predominant hydrochemical process within the mentioned wells.

Moreover, the stratigraphic factors, such as clay strata, may have isolated fresh groundwater from seawater. The origin of salinity may also be explained by the Gibbs diagrams: evapotranspiration (ET) and rock-water interaction play an important role to the increase of groundwater salinity.

The cation exchange processes are in progress since, calcium and magnesium are in excess of bicarbonate and sulphates. Finally, high correlation between the sulphates and sodium may indicate dissolution of evaporites relics.

8. References

Chadha, D.K.A., 1999. Proposed new diagram for geochemical classification of natural waters and interpretation of chemical data, *Hydrogeology Journal*, 7(5), 431–439.

Christides, A., Mavrakis A., Mitilineou A., 2011. A case of intense seawater intrusion to aquifer of the Thriasio Plain. Greece, *Proceedings of the 12th International Conference on Environmental Science and Technology (12th ICEST)*, vol B: 152-159.

Dimitriou, E., Mentzafou, A., et al. 2011. Monitoring of the ecological quality of Koumoundourou Lake and designing of management, restoration and development actions. 2nd Technical report, IIWHCMR, p. 310.

Dounas, A, 1971. The geology between Megara and Erithres area, PhD National and Kapodistrian University of Athens (in Greek), 141 p.

Dounas, A., Panagiotides G., 1964. Precursor report on the hydrogeological conditions of Thriassion. Institute of Geology and Subsurface Research, Athens (in Greek) 28 p.

Foumelis, M., 2019. Velocity field and crustal deformation of broader Athens plain (Greece) from dense network. *Journal of Applied Geodesy*, 13 (4), 305-316.

Ganas, A., Pavlides, SB., Sboras, S., Valkaniotis, S. Papaioannou, S., Alexandris, G.A., Plessa, A. Papadopoulos, G.A., 2004. Active fault geometry and kinematics in Parnitha Mountain, Attica, Greece. *Journal of Structural Geology*, 26 (11), 2103-2118.

Gibbs, R.J., 1971. Mechanisms controlling world water chemistry. *Sci J*, 172 (3), 870-872.

Goumas, G., 2006. Investigation of the structure of Thriassion Plain based on geophysics, MSc thesis, University of Athens pp 190.

Hermides, D., 2018. Hydrogeological conditions of the Thriassion Plain basin with emphasis on the geohydraulic characteristics of the aquifers and the groundwater quality. PhD thesis, Agricultural University of Athens, pp 283.

Hermides, D., Stamatis, G., 2017. Origin of halogens and their use as environmental tracers in aquifers of Thriassion Plain, Attica, Greece. *Environ Earth Sci.*, 76, 306. https://doi.org/10.1007/s12665-017-6611-z

Hermides, D., Mimides, T., Stamatis, G., 2016. Contribution to hydraulic characteristics of plio-pleistocene deposits of Thriassion plain of Attica, *Bul. Geol. Soc. Greece*, 50 (2), 967-976, doi: http://dx.doi.org/10.12681/bgsg.11801

Iliopoulos, G., Stamatis, G., Stournaras, G., 2010. Marine and human activity effects on the groundwater quality of Thriassion Plain, Attica, Greece Proceedings of the 9th International Hydrogeological Congress of Greece, 2, 409-416.

Kambouroglou, E., 1989. Eretria paleogeographic and geomorphological evolution during Holocene relationship of the natural environment and ancient settlements, PhD thesis National and Kapodistrian University of Athens, pp 493.

Kaminari, M.A., 1994. Geochemical pilot survey of the lands of the wider region of Eleusis (Thriassion Plain) to detect pollution from heavy metals, IGME, Athens.

Katsikatsos, G., Mettos, A., Vidakis, M., Dounas, A., Pomoni, F., Tsaila-Monopolis, S., Skourtsi-Koroneou, V., 1986. Geological map of Greece, in scale 1:50.000, ‘‘Athina-Elefsis’’ sheet, IGME publication, Athens.

Kounis, G., Siemos N., 1990. Hydrogeological research of the aquifers of Thriassion Plain, for the water supply of Hellenic Refinery (In Greek), IGME, Athens, pp 39.

Kraft, J., Kayan I., Erol O., 1980 Geomorphic reconstructions in the environs of ancient Troy, *Science* 209, (4458), 776-782.

Lambeck, K., 1996. Sea level change and shore-line evolution in Aegean Greece since Upper Palaeolithic time. *Antiquity*, 70, (269), 588–611.

Lioni, A., Stournaras G., Stamatis G., 2008. Degradation of Groundwater quality of Thriassion Plain through Natural Factors and human activity, Proceedings of the 8th Hydrogeological Congress of Greece, 2, 577-586.

Makri, P. 2008. Investigating the pollution from BTEX in the groundwater of Thriassion Plain, PhD National and Kapodistrian University of Athens, pp 260.

Mariolakos, H., Theocharis, D., 2001. Shifting shores in the Saronic Gulf during the last 18,000 years and the Kychreia paleolimni. Proceedings of the 9th International Conference, Athens, *Bul. Geol. Soc. Greece*, XXXVI, 1, 405-413.

Mariolakos, H., Fountoulis, I., Sideris, C., Chatoupis, T., 2001. Morphoneotectonic structure of Parnes' Mt of Attica Proceedings of the 9th International Congress, Athens, *Bul. Geol. Soc. Greece, XXIV*/1, 183-190.

Mimides, Th., 2002. Pollution Source and suggestions on environmental upgrading of Lake Koumoundourou. Environmental Impact Study, Agricultural University of Athens, for the Prefecture of Western Attica (in Greek), 22 p.

Paraschoudes, B., 2002. Hydrogeological study of western Attica (Megara-Thriassio Field). Ministry of Agriculture, Athens 165 p.

Skianis, G., Noutsis B., 2008. Geophysics study in Thriassion Plain. IGME, Athens (in Greek), 176 p.

Zacharias, A., Sarandakos K., Andre C., 2003. Report on sample drilling and Morphotectonics study in the area around Koumoundourou Lake, 2nd Technical Report, Hellenic Center of Marine Research (ELKETHE) /IIW, Anavyssos Attica, 72p.